

Natural Convection Heat Transfer from an Inclined Cylinder

Aubrey G. Jaffer and Martin S. Jaffer
e-mail: agj@alum.mit.edu

Abstract

This investigation derives a novel formula predicting the natural convective heat transfer from an inclined cylinder given its length, diameter, inclination angle, Rayleigh number, and the fluid's Prandtl number and thermal conductivity.

The present formula was tested with 93 inclined cylinder measurements having length-to-diameter ratios between 1.48 and 104 in nine data-sets from three peer-reviewed studies, yielding (data-set) root-mean-squared relative error values between 1.6% and 4.7%.

This research did not receive any specific grant from funding agencies in the public, commercial, or not-for-profit sectors.

Table of Contents

1. <i>Introduction</i>	1
2. <i>Data-Sets and Evaluation</i>	3
3. <i>Theory from Prior Works</i>	5
4. <i>Natural Convection</i>	6
5. <i>Inclination</i>	12
6. <i>Discussion</i>	15
7. <i>Conclusions</i>	16
8. <i>Nomenclature</i>	16
9. <i>References</i>	17

1. Introduction

Natural convection is the flow caused by nonuniform density in a fluid under the influence of gravity. Natural convection is a fundamental process with application from engineering to geophysics.

Changes in fluid density can be caused by changes in temperature or solute concentration. Under the influence of gravity, density changes cause fluid flow, which also transports heat or solute. Rates of transfer grow until reaching a plateau. This investigation seeks to predict the overall steady-state heat transfer rate from an external, cylindrical, isothermal surface inclined at any angle in a Newtonian fluid.

An “external” surface is one that fluid can flow around freely, especially horizontally. If enclosed, the enclosure must have dimensions much larger than the heated or cooled surface.

Jaffer [1] derived a natural convection formula for external flat plates (with convex perimeter) in any orientation from its analyses of horizontal and vertical plates. This investigation uses the same approach.

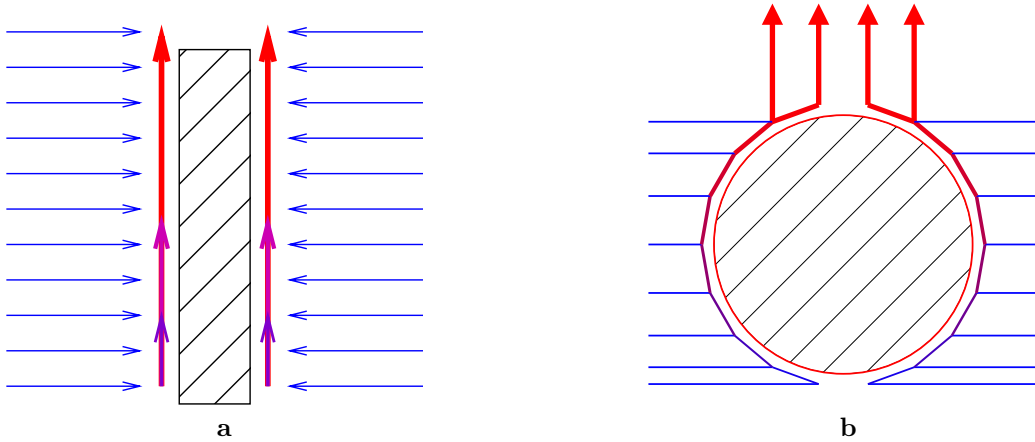


Figure 1 Induced flow around cylinder (a) vertical (b) level

1.1 Flow Topologies. There are two topologies of convective flow from external, convex cylinders. Figure 1 shows the induced fluid flows around heated vertical and horizontal cylindrical surfaces.

An important aspect of both flow topologies is that fluid is pulled horizontally before being heated by the cylinder. Pulling horizontally expends less energy than pulling vertically because the latter does work against the gravitational force. Inadequate horizontal clearance around a cylinder can obstruct flow and reduce convection and heat transfer.

There is a symmetry in external natural convection; a cooled cylinder induces downward flow instead of upward flow. The rest of this investigation assumes that the cylindrical exterior surface is warmer than the fluid.

1.2 Turbulence. Jaffer [1] derives the formula for an external flat surface’s total natural convective heat transfer from the thermodynamic constraints on heat-engine efficiency. The fundamental laws of thermodynamics make no distinction between laminar and turbulent flows. Thus, a single formula governs both laminar and turbulent natural convection (Fujii and Imura [2] Churchill and Chu [3], Jaffer [1]).

1.3 Characteristic Length. The characteristic length L is the length scale of a physical system. As with a vertical rectangular plate, a vertical cylinder’s characteristic length is its height.

The characteristic length of a level circular cylinder is its diameter d . More general is the hydraulic diameter $d = 4L^*$, which is 4 times the area-to-perimeter ratio of the cylinder’s cross-section. Note that for circular cylinders they are the same.

1.4 Fluid Mechanics. In engineering, convection heat transfer rates are expressed using the average surface conductance \bar{h} with units $W/(m^2 \cdot K)$.

In fluid mechanics, the convective heat transfer rate is represented by the dimensionless average Nusselt number ($\overline{Nu} \equiv \bar{h}L/k$), where k is the fluid’s thermal conductivity with units $W/(m \cdot K)$, and L is the system’s characteristic length (m).

The Rayleigh number Ra is the impetus for fluid flow due to gravity acting on density differences caused by temperature. A fluid’s Prandtl number Pr is its momentum diffusivity per thermal diffusivity ratio. For mass transfer, the fluid’s Schmidt number Sc is analogous; Pr will be used in formulas.

When rising convection induced fluid flow must pass along or around the object’s surface, Ra is scaled by a “self-obstruction” factor $1/\Xi$, which depends only on Pr . This applies to both cylinder flow topologies.

The system’s characteristic length L scales \overline{Nu} , while L^3 scales Ra . Variables Ξ , \bar{h} , Pr , and Sc are independent of L .

1.5 Combining Transfer Processes. Formula (1) is an unnamed form for combining functions which appears frequently in heat or mass transfer formulas:

$$F^p = F_1^p + F_2^p \quad (1)$$

Churchill and Usagi [4] stated that such formulas are “remarkably successful in correlating rates of transfer for processes which vary uniformly between these limiting cases.” Convection transfers heat (or solute) between the cylinder and the fluid.

1.6 The ℓ^p -norm. When $F_1 \geq 0$ and $F_2 \geq 0$, taking the p th root of both sides of Equation (1) yields a vector-space functional form known as the ℓ^p -norm, which is notated $\|F_1, F_2\|_p$:

$$\|F_1, F_2\|_p \equiv [|F_1|^p + |F_2|^p]^{1/p} \quad (2)$$

Norms generalize the notion of distance. Formally, a vector-space norm obeys the triangle inequality: $\|F_1, F_2\|_p \leq |F_1| + |F_2|$, which holds only for $p \geq 1$. However, $p < 1$ is also useful.

When $p > 1$, the processes modeled by F_1 and F_2 compete and $\|F_1, F_2\|_p \geq \max(|F_1|, |F_2|)$; the most competitive case is $\|F_1, F_2\|_{+\infty} \equiv \max(|F_1|, |F_2|)$.

The ℓ^1 -norm models independent processes; $\|F_1, F_2\|_1 \equiv |F_1| + |F_2|$.

When $0 < p < 1$, the processes cooperate and $\|F_1, F_2\|_p \geq |F_1| + |F_2|$. Cooperation between conduction and flow-induced heat transfer occurs in some natural convection systems.

2. Data-Sets and Evaluation

Heat transfer measurements were captured from graphs in the cited works by measuring the distance from each point to its graph’s axes, then scaling to the graph’s units using the “Engauge” software (version 12.1).

Churchill and Chu [5] collected level cylinder (angle $\vartheta = 0^\circ$) heat and mass transfer measurements from eleven studies spanning more than 23 orders of magnitude of Ra . The Kutateladze [6] data-set (with the largest Ra values) is treated separately in Table 1.

Al-Arabi and Khamis [7] measured natural convection heat transfer from a cylinder at six angles. They measured local temperatures along the cylinder, but incorrectly inferred the average heat transfer.

Popiel, Wojtkowiak, and Bober [8] measured natural convection heat transfer from four vertical cylinders with $1 < H/d < 59$. Unfortunately, they tested with the bottom of the cylinder resting directly on a flat platform, which would impede horizontal fluid flow at the bottom. Extra walls were found to significantly affect convective heat transfer in Jaffer [1].

Goldstein, Khan, and Srinivasan [9] measured natural convection mass transfer from three cylinders at four inclinations.

Heo and Chung [10] measured natural convection mass transfer from five cylinders with $3.7 < H/d \leq 25$ at inclinations $0^\circ \leq \vartheta \leq 90^\circ$.

Table 1 Cylinder Natural convection data-sets

Source	Study		ϑ	$Ra_d/\Xi_\bullet \geq$	$Ra_d/\Xi_\bullet \leq$	\pm	#
Churchill & Chu [5]	Kutateladze [6]		0°	2.8×10^9	3.4×10^{12}		6
Churchill & Chu [5]	10 others		0°	7.5×10^{-12}	3.3×10^9		57
Source	Pr or Sc	H/d	ϑ	$Ra/L^3 \geq$	$Ra/L^3 \leq$	\pm	#
Goldstein et al. [9]	2300	0.63-2.34	0°	3.2×10^{13}	1.6×10^{14}		4
Goldstein et al. [9]	2300	0.63-2.34	30°	1.4×10^{13}	3.2×10^{14}		11
Goldstein et al. [9]	2300	0.63-2.34	60°	6.8×10^{12}	4.4×10^{14}		11
Goldstein et al. [9]	2300	0.63-2.34	90°	2.3×10^{12}	6.1×10^{14}		16
Heo & Chung [10]	2094	25	$0^\circ\text{--}90^\circ$	1.3×10^{14}	1.3×10^{14}		13
Heo & Chung [10]	2094	7.4	$0^\circ\text{--}90^\circ$	1.7×10^{14}	1.7×10^{14}		13
Heo & Chung [10]	2094	3.7	$0^\circ\text{--}90^\circ$	1.7×10^{14}	1.7×10^{14}		13
Heo & Chung [10]	2094	13	$0^\circ\text{--}90^\circ$	1.7×10^{14}	1.7×10^{14}		9
Heo & Chung [10]	2094	6.7	$0^\circ\text{--}90^\circ$	1.7×10^{14}	1.7×10^{14}		9
AlArabi & Khamis [7]	0.708	15.5–104	0°	4.8×10^9	4.8×10^9		7
AlArabi & Khamis [7]	0.708	15.5–104	30°	4.8×10^9	4.8×10^9		7
AlArabi & Khamis [7]	0.708	15.5–104	45°	4.8×10^9	4.8×10^9		7
AlArabi & Khamis [7]	0.708	15.5–104	60°	4.8×10^9	4.8×10^9		7
AlArabi & Khamis [7]	0.708	15.5–104	75°	4.8×10^9	4.8×10^9		7
AlArabi & Khamis [7]	0.708	15.5–104	90°	4.8×10^9	4.8×10^9		7

2.1 Not Empirical. Empirical theories derive their coefficients from measurements, inheriting the uncertainties from those measurements. Theories developed from first principles derive their coefficients mathematically. For example, Incropera, DeWitt, Bergman, and Lavine [11] (p. 210) gives the thermal conductance (units W/K) of a diameter d sphere ($L_s = d/2$) into an unbounded stationary, uniform medium having thermal conductivity k as:

$$U_0 = 2\pi dk \quad (3)$$

The present theory predicting natural convective heat transfer from a round cylindrical surface derives from first principles; it is not empirical. Each formula is tied to aspects of the cylinder geometry and orientation, fluid, and flow.

2.2 RMS Relative Error. Root-mean-squared (RMS) relative error (RMSRE) provides an objective, quantitative evaluation of theory versus experimental data. It gauges the fit of measurements $g(Re_j)$ to function $f(Re_j)$, giving each of the n samples equal weight in Formula (4). Along with presenting RMSRE, charts in the present work split RMSRE into the bias and scatter components defined in Formula (5). The root-sum-squared of bias and scatter is RMSRE.

$$\text{RMSRE} = \sqrt{\frac{1}{n} \sum_{j=1}^n \left| \frac{g(Re_j)}{f(Re_j)} - 1 \right|^2} \quad (4)$$

$$\text{bias} = \frac{1}{n} \sum_{j=1}^n \left\{ \frac{g(Re_j)}{f(Re_j)} - 1 \right\} \quad \text{scatter} = \sqrt{\frac{1}{n} \sum_{j=1}^n \left| \frac{g(Re_j)}{f(Re_j)} - 1 - \text{bias} \right|^2} \quad (5)$$

3. Theory from Prior Works

Subscripts and variable names are not uniform among prior works; they have been renamed consistently for inclusion in the present work. Where possible, the formulas are written using the ℓ^p -norm.

3.1 Vertical Cylinder. Sparrow and Gregg [12] and Cebeci [13] created differential equations modeling the thermal boundary layer surrounding a vertical cylinder. Solved numerically, they created graphs and tables relating the cylinder's local temperature profiles to a that of a vertical plate having the same height. Sparrow and Gregg's graphs only address $Pr = 0.71$ and $Pr = 1$; Cebeci expanded the range to $0.01 < Pr < 100$.

Popiel et al. [8] fits a complicated formula to numerical solutions of the Cebeci [13] equations. Of greater interest is a simple formula (similar to the vertical plate formula from Churchill and Chu [3]) that they attribute to S. M. Yang [14]:

$$\left\| 0.36 \frac{H}{d}, 0.150 \sqrt[3]{\frac{Ra_H}{\|1, 0.492/Pr\|_{9/16}}} \right\|_{1/2} \quad (6)$$

$\|1, 0.492/Pr\|_{9/16}$ is the denominator used for a vertical plate in Churchill and Chu [3]. Jaffer [1] finds that $\|1, 0.5/Pr\|_{\sqrt{1/3}}$ is more accurate.

3.2 Level Cylinder. Formula (7) is the ℓ^p -norm form of what Churchill and Chu [5] propose as the natural convective \overline{Nu}_d from a level diameter d isothermal cylinder (excluding end faces).

$$\left\| 0.36, 0.150 \sqrt[3]{\frac{Ra_d}{\|1, 0.559/Pr\|_{9/16}}} \right\|_{1/2} \quad (7)$$

They also propose a laminar flow formula with an exponent of $1/4$ instead of $1/3$:

$$0.36 + 0.518 \sqrt[4]{\frac{Ra_d}{\|1, 0.559/Pr\|_{9/16}}} \quad (8)$$

The denominator $\|1, 0.559/Pr\|_{9/16}$ differs from $\|1, 0.492/Pr\|_{9/16}$ only in its coefficient, which is within 1% of $9/16$. This investigation uses $\|1, \sqrt{1/3}/Pr\|_{\sqrt{1/3}}$ as denominator for level cylinders.

3.3 Inclined Cylinder. AlArabi and Khamis [15] propose a limited range formula to match their local heat transfer measurements:

$$Nu_H = 0.60 - 0.488 [\cos \vartheta]^{1.03} \exp_{Ra_H} \left(\frac{1}{4} + \frac{[\cos \vartheta]^{1.75}}{12} \right) \quad (9)$$

$$Ra_H < 1.48 \times 10^8 + 4.5 \times 10^8 / \tan \vartheta \quad Pr = 0.71$$

where the notation $\exp_b(\varphi) \equiv b^\varphi$.

Goldstein et al. [9] propose a formula to match their mass transfer convection measurements using an angle-dependent characteristic-length G :

$$\overline{Sh}_G = 0.712 Ra_G^{1/4} \quad G = \frac{H \sin \vartheta + d \cos \vartheta}{(\sin \vartheta + \cos \vartheta)^{7/3}} \quad (10)$$

where \overline{Sh} is the (average) Sherwood number, an analog of the (average) Nusselt number \overline{Nu} .

4. Natural Convection

First, a review of flat surface convection: From thermodynamic constraints, Jaffer [1] derives generalized natural convection Formula (11) with the parameters specified in Table 2:

$$\overline{Nu} = \left\| Nu_0 [1 - C], {}^{2+E}\sqrt{[C D Nu_0]^{3+E} \frac{2}{B} Ra} \right\|_p \quad (11)$$

$$\Xi = \left\| 1, \frac{1/2}{Pr} \right\|_{\sqrt{1/3}} \quad Nu_0^* = \frac{2}{\pi} \approx 0.637 \quad Nu_0' = \frac{2^4}{\sqrt[4]{2} \pi^2} \approx 1.363 \quad (12)$$

Table 2 Plate natural convection parameters

Face	θ	L	\overline{Nu}	Nu_0	Ra	B	C	D	E	p
up	-90°	L^*	\overline{Nu}^*	Nu_0^*	Ra^*	2	$1/\sqrt{8}$	1	1	$1/2$
vertical	0°	L'	\overline{Nu}'	Nu_0'	Ra'/Ξ	$1/2$	$1/2$	$1/4$	1	$1/2$
down	$+90^\circ$	L_R	\overline{Nu}_R	$Nu_0'/2$	Ra_R/Ξ	4	$1/2$	2	3	1

- θ is the angle of the plate from vertical; $\theta = +90^\circ$ is face down;
- L is the characteristic length of a flat plate with convex perimeter:
 - face up ($\theta = -90^\circ$) L^* is the area-to-perimeter ratio;
 - * For a $Y \times Z$ rectangle, $L^* = YZ/[2Y + 2Z]$.
 - * For a diameter d disk, $L^* = d/4$.
 - vertical ($\theta = 0^\circ$) L' is the harmonic mean of the perimeter vertical spans;
 - * Given a convex vertical plate with maximum width W whose vertical span at horizontal offset w is $H(w)$:

$$L' = W \left/ \int_0^W \frac{1}{H(w)} dw \right. \quad (13)$$

- * For a diameter d disk, $L' = 2d/\pi$.
- * For a level height H rectangle, $L' = H$.
- face down ($\theta = +90^\circ$) L_R is the harmonic mean of the perimeter distances to that bisector which is perpendicular to the shortest bisector;
 - * Given a flat surface with convex perimeter defined by functions $H_+(w) > 0$ and $H_-(w) < 0$ within the range $0 < w < W$ along the equal-area bisector which is perpendicular to the shortest equal-area bisector:

$$L_R = 4W \left/ \int_0^W \left[\frac{1}{|H_+(w)|} + \frac{1}{|H_-(w)|} \right] dw \right. \quad (14)$$

- * For a $Y \times Z$ rectangle, $L_R = \min(Y, Z)/2$.
- * For a diameter d disk, $L_R = d/\pi$.
- Nu_0 is the dimensionless conduction into motionless fluid;
- Ra' is computed with vertical L' ; $Ra^* = Ra' [L^*/L']^3$; $Ra_R = Ra' [L_R/L']^3$.
 Pr does not affect upward-facing heat transfer because the heated fluid flows directly upward, as does conducted heat. When heated fluid must flow along vertical and downward-facing plates, its heat transfer potential is reduced by dividing Ra by Ξ from Formula (12).
- B is the sum of the mean lengths of flows tangent to a wall or counter-flow on one side divided by L ;
- C is the surface area fraction responsible for flow induced heat transfer;
- D is the effective length of heat transfer contact with one side of the plate divided by L ;
- E is the count of 90° changes in direction of thermally induced fluid flow;
- The ℓ^p -norm combines the static conduction and induced convective heat flows.

4.1 Cylinder. Formula (11) is not limited to flat surfaces. Natural convection heat transfer from a cylinder can be modeled using Formula (11) with the parameters in Table 3. The angle from horizontal is ϑ .

Table 3 Cylinder natural convection parameters

Cylinder	ϑ	L	\overline{Nu}	Nu_0	Ra	B	C	D	E	p
level	0°	d	\overline{Nu}_\bullet	Nu_0^\bullet	Ra_d/Ξ_\bullet	$\pi/2$	$1/2$	$\pi/3$	E^\bullet	$1/3$
vertical	90°	H	\overline{Nu}_\parallel	$Nu_0^\bullet \frac{H}{d}$	Ra_H/Ξ	1	$1/2$	$\frac{1}{6}[\frac{d}{H}]^{5/4}$	1	$1/6$

- The height H of a vertical cylinder is its characteristic length.

The diameter d of a level circular cylinder is its characteristic length. This investigation uses the hydraulic diameter, which is 4 times the area-to-perimeter ratio of the cylinder's cross-section, as d . Note that for circular cylinders they are the same.

- Conduction shape factors are not well-defined with unbounded source areas, but Nusselt numbers can be. A cylinder's Nu_0 (conduction into static fluid) must distribute in two dimensions what the sphere distributes in three. Using Formula (3) U_0 and $L_s = d/2$:

$$Nu_0^\bullet = \left[\frac{U_0 L_s}{\pi d^2 k} \frac{L_s}{d} \right]^{3/2} = 2^{-3/2} \approx 0.354 \quad (15)$$

which is different from the 0.36 value in prior works Formulas (6), (7) and (8).

The vertical cylinder's conduction is the same as a level cylinder. But its characteristic length is H , not d . Consequently vertical $Nu_0 = Nu_0^\bullet H/d$ as per S. M. Yang [14] in Formula (6).

- Ra_H is computed with vertical H ; $Ra_d = Ra_H [d/H]^3$.

Ra_H is divided by Formula (12) $\Xi(Pr)$ as with a vertical plate. The upper part of the level cylinder is unobstructed; its Ra_d divisor must be between the 1 of an upward facing plate and the Ξ of a vertical plate. So Ra_d should be divided by Formula (16) Ξ_\bullet . Both $1/\Xi_\bullet$ and $1/\Xi$ are plotted in Figure 2.

$$\Xi_\bullet = \left\| 1, \frac{\sqrt{1/3}}{Pr} \right\|_{\sqrt{1/3}} \quad \Xi = \left\| 1, \frac{1/2}{Pr} \right\|_{\sqrt{1/3}} \quad (16)$$

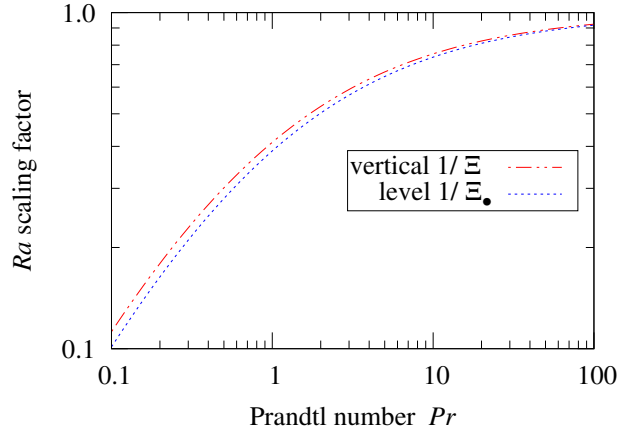


Figure 2 Ra scaling factors

- Fluid rises the full height of the vertical cylinder; it has $B = 1$.

Fluid flows tangent to the horizontal cylinder over (each) half of its perimeter in Figure 1b; $B = \pi/2$.

- $C = 1/2$ because fluid flow with both cylinder orientations is two-dimensional.
- The vertical plate's $D = 1/4$ because fluid flowing by the upper half is already heated and accelerating upward. The vertical cylinder lacks vertical edges adjacent to unheated fluid; Relative to H , only a short length of the vertical cylinder heats a significant amount of fluid:

$$D = \frac{1}{6} \left[\frac{d}{H} \right]^{5/4} \quad (17)$$

Most heat transfer occurs where the level cylinder's surface is vertical or downward-facing, not upward-facing. Two thirds of $B = \pi/2$ is $D = \pi/3$.

- Fluid flow induced by a vertical cylinder experiences one 90° change in direction; its $E = 1$.

Figure 1b shows convecting fluid flowing tangent to the lower half of a level cylinder. For a unit radius cylinder, fluid flowing horizontally at elevation $0 < y < 1$ must bend $\pi - \arcsin(y)$ radians upward in order to be tangent to the cylinder. The average angle is:

$$\int_0^1 \pi - \arcsin y \, dy = 1 + \frac{\pi}{2} \approx 2.571 \text{ rad} \quad (18)$$

Fluid at mid-height is already moving upward; it requires no more bend. Fluid moving tangent to the upper part of a cylinder will require some bend, but less fluid is flowing tangent to the cylinder at the top; so $\arcsin x$ is weighted by x^2 , where x is the distance from the vertical mid-line:

$$\int_0^1 \frac{\pi}{2} - x^2 \arcsin x \, dx = \frac{2+3\pi}{9} \approx 1.269 \text{ rad} \quad (19)$$

Averaging the bends of the upper and lower halves divided by $\pi/2$:

$$E^\bullet = \frac{1}{2} + \frac{1}{\pi} + \frac{1}{3} + \frac{2}{9\pi} \approx 1.222 \quad (20)$$

- The static conduction and induced convective heat flows of a vertical cylinder cooperate more than from a vertical plate; they combine as the $\ell^{1/6}$ -norm. The level cylinder flows combine as the $\ell^{1/3}$ -norm.

4.2 Surface Conductance Formulas. Because the characteristic lengths scaling \overline{Nu}^* , \overline{Nu}' , and \overline{Nu}_R can be different, combining plate convections works in terms of scale-free \overline{h}^* , \overline{h}' , and \overline{h}_R :

$$\overline{h}^* = \frac{k}{L^*} \left\| Nu_0^* \left[1 - \sqrt{\frac{1}{8}} \right], \frac{Nu_0^{*4/3}}{4} \sqrt[3]{Ra^*} \right\|_{1/2} \approx \frac{k}{L^*} \left\| 0.411, 0.137 \sqrt[3]{Ra^*} \right\|_{1/2} \quad (21)$$

$$\overline{h}' = \frac{k}{L'} \left\| \frac{Nu_0'}{2}, \frac{Nu_0'^{4/3}}{8 \sqrt[3]{2}} \sqrt{\frac{Ra'}{\Xi}} \right\|_{1/2} \approx \frac{k}{L'} \left\| 0.682, 0.150 \sqrt{\frac{Ra'}{\Xi}} \right\|_{1/2} \quad (22)$$

$$\overline{h}_R = \frac{k}{L_R} \left\| \frac{Nu_0'}{4}, \frac{Nu_0'^{6/5}}{2^{7/5}} \sqrt[5]{\frac{Ra_R}{\Xi}} \right\|_1 \approx \frac{k}{L_R} \left[0.341 + 0.550 \sqrt[5]{\frac{Ra_R}{\Xi}} \right] \quad (23)$$

Formulas (24) and (25) model horizontal and vertical cylinders, respectively.

$$\overline{h}^\bullet = \frac{k}{d} \left\| \frac{Nu_0^\bullet}{2}, \sqrt[2+E^\bullet]{\left[\frac{\pi Nu_0^\bullet}{6} \right]^{3+E^\bullet} \frac{Ra_d}{\pi \Xi_\bullet}} \right\|_{1/3} \approx \frac{k}{d} \left\| 0.177, 0.118 \left[\frac{Ra_d}{\Xi_\bullet} \right]^{0.310} \right\|_{1/3} \quad (24)$$

$$\overline{h}_\parallel = \frac{k}{H} \left\| \frac{Nu_0^\bullet}{2} \frac{H}{d}, \sqrt[3]{\left[\frac{Nu_0^\bullet}{12} \right]^4 \frac{d}{H} \frac{2 Ra_H}{\Xi}} \right\|_{1/6} \approx \frac{k}{H} \left\| 0.177 \frac{H}{d}, 0.0115 \sqrt[3]{\frac{d}{H} \frac{Ra_H}{\Xi}} \right\|_{1/6} \quad (25)$$

4.3 End-Caps. The flow modes of each end-cap (upper and lower, respectively) compete as the ℓ^{16} -norm:

$$\overline{h}_\uparrow = \left\| \overline{h}'(\cos \vartheta Ra_H), \frac{\overline{h}^*(\sin \vartheta Ra^*)}{1 + H/d} \right\|_{16} \quad \overline{h}_\downarrow = \left\| \overline{h}'(\cos \vartheta Ra_H), \frac{\overline{h}_R(\sin \vartheta Ra_R)}{1 + H/d} \right\|_{16} \quad (26)$$

where $L' = 2d/\pi$, $L^* = d/4$, and $L_R = d/\pi$. The $1 + H/d$ denominator models the reduction of vertical cylinder heat transfer by already heated fluid. The trigonometric functions of ϑ are explained in Section 5.

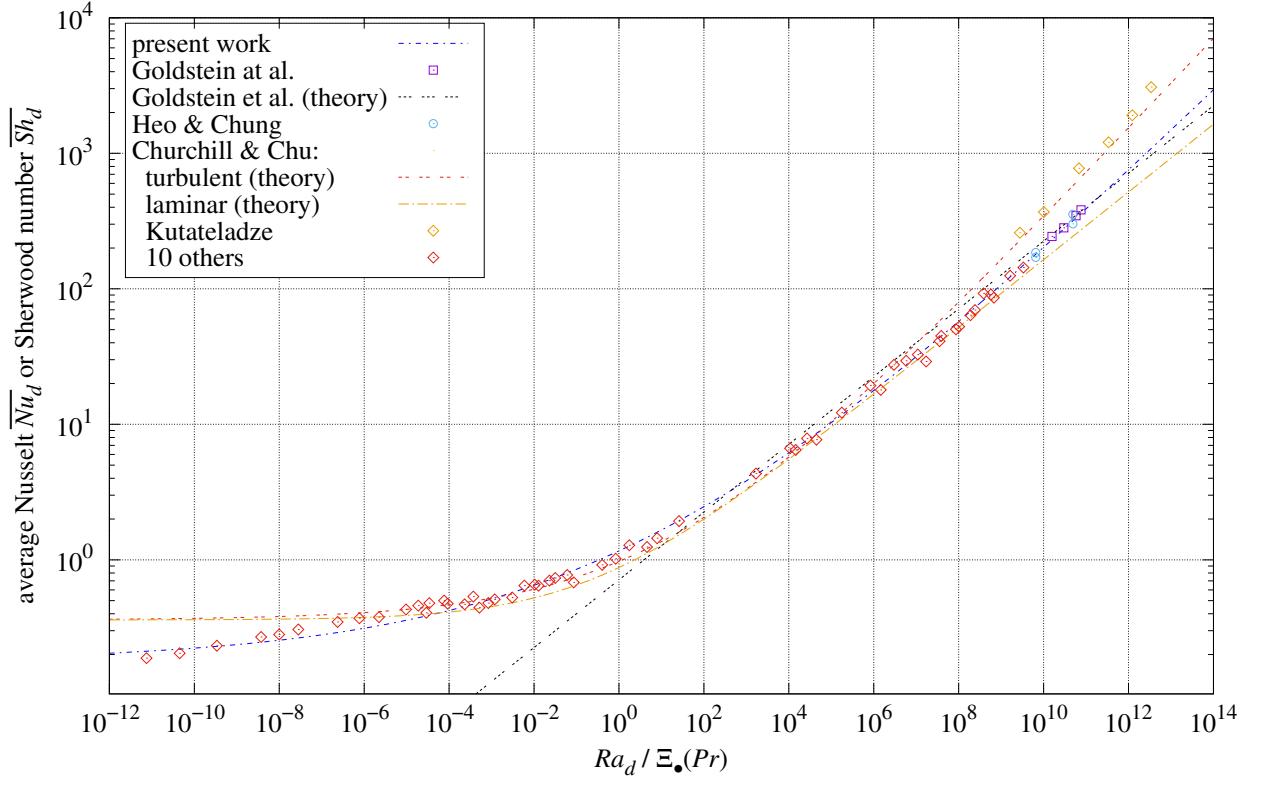


Figure 3 Natural convection from level cylinder

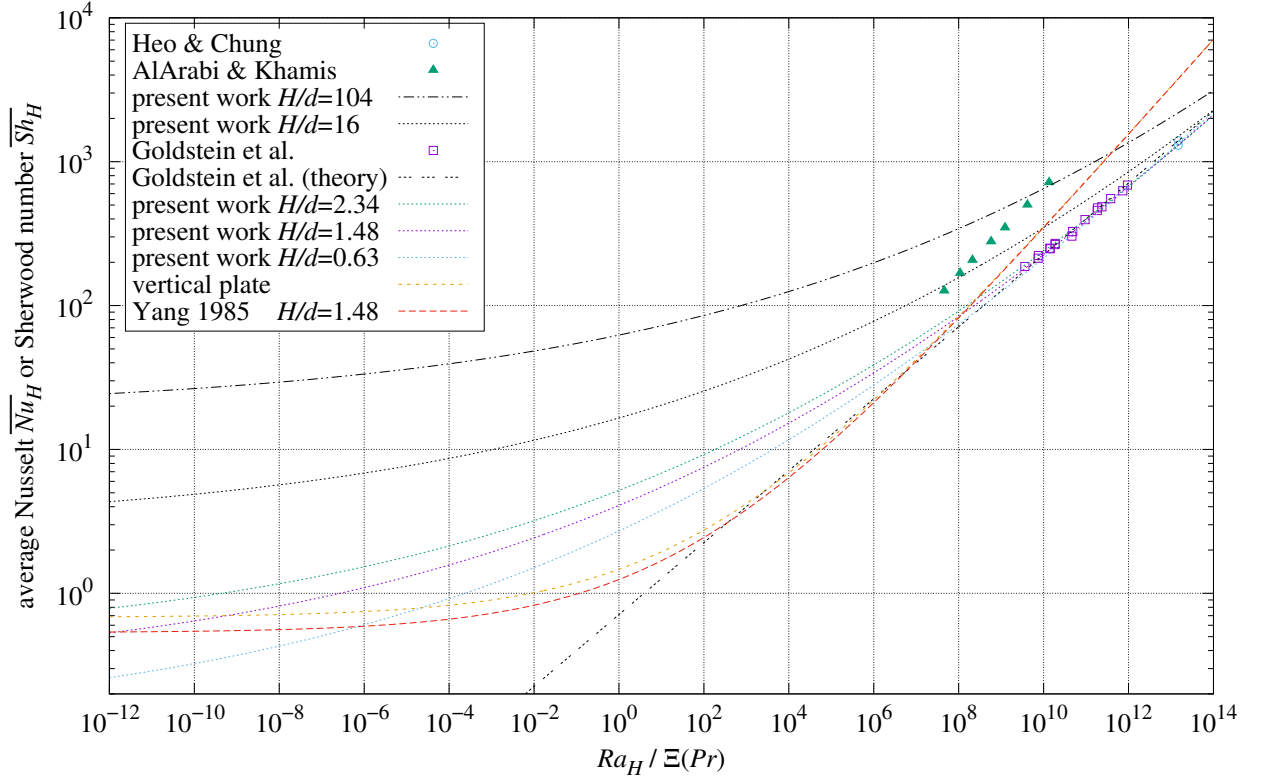


Figure 4 Natural convection from vertical cylinder

4.4 Comparison With Level Cylinder Measurements. Figure 3 compares four level cylinder theories with data-sets from Churchill and Chu [5], Goldstein et al. [9], and Heo and Chung [10].

- The “Churchill & Chu: turbulent (theory)” trace is Formula (7).
- The “Churchill & Chu: laminar (theory)” trace is Formula (8).
- The “Goldstein et al. (theory)” trace is Formula (10).
- The “present work” trace is $\overline{Nu}_\bullet = \overline{h}_\bullet d/k$, where \overline{h}_\bullet is Formula (24).

Table 4 presents statistics of the Churchill and Chu data-set measurements versus their turbulent Formula (7), laminar Formula (8), and with the present work’s Formula (24).

The six point data-set which Churchill and Chu [5] attribute to Kutateladze [6] is clearly outlying, exceeding all the traces. The remaining ten of the Churchill and Chu data-sets, spanning more than 20 orders-of-magnitude of Ra/Ξ_\bullet , have 11% RMSRE versus the present theory in Table 4, a significant improvement from Formula (7)’s 21% RMSRE and Formula (8)’s 19% RMSRE.

Table 4 Churchill and Chu data-sets versus theories

Study	Theory	$Ra_d/\Xi_\bullet \geq$	$Ra_d/\Xi_\bullet \leq$	RMSRE	Bias	Scatter	#
Kutateladze [6]	present	2.8×10^9	3.4×10^{12}	125.8%	−120.9%	34.8%	6
10 others	turbulent	7.5×10^{-12}	3.3×10^9	21.1%	+9.8%	18.7%	57
10 others	laminar	7.5×10^{-12}	3.3×10^9	19.0%	−7.9%	17.2%	57
10 others	present	7.5×10^{-12}	3.3×10^9	10.9%	−1.5%	10.8%	57

In Table 5 the Goldstein et al. [9] and Heo and Chung [10] data sets have RMSRE values smaller than 4%. Partially overlapping the Kutateladze [6] data-set’s Ra/Ξ_\bullet range, they provide further evidence justifying its exclusion. The “Goldstein et al. (theory)” trace matches its own level cylinder data with 3.5% RMSRE, but is unusable at $Ra/\Xi_\bullet < 1$.

Table 5 Level cylinder measurements versus present theory

Source	Pr or Sc	H/d	ϑ	RMSRE	Bias	Scatter	#
Goldstein et al. [9]	2300	1.48	0°	4.7%	−4.4%	1.6%	4
Heo & Chung [10]	2094	3.73–13.2	0°	1.6%	+0.0%	1.6%	4

4.5 Comparison With Vertical Cylinder Measurements. Figure 4 compares four vertical cylinder theories with data-sets from AlArabi and Khamis [15], Goldstein et al. [9], and Heo and Chung [10].

- The “vertical plate” trace is $\overline{Nu}' = \overline{h}' L'/k$, where \overline{h}' is Formula (22).
- The “Yang 1985” trace is Formula (6).
- The “Goldstein et al. (theory)” trace is Formula (10).
- The “present work” traces are $\overline{Nu}^\parallel = \overline{h}^\parallel H/k$, where \overline{h}^\parallel is Formula (25).

Table 6 presents vertical statistics of the inclined cylinder data-sets. Comparing vertical cylinder heat transfer measurements is more difficult than with level cylinders because the surface conductance depends on H/d , the height-to-diameter ratio.

The “Goldstein et al. (theory)” trace matches its own level cylinder data with 3.6% RMSRE. However, the cylinder diameter d does not affect the “Goldstein et al. (theory)” Formula (10) when the cylinder is vertical. Its RMSRE for vertical AlArabi and Khamis cylinders exceeds 100%.

While the other formulas all raise $Ra_H^{1/3}$, the gentle curvature of the $\ell^{1/6}$ -norm dominates the slopes of “present work” traces through the entire range of Figure 4. This indicates that vertical plate convection is rarely a good approximation for vertical cylinder convection.

Table 6 Vertical cylinder measurements versus present theory

Source	Pr or Sc	H/d	ϑ	RMSRE	Bias	Scatter	#
Goldstein et al. [9]	2300	1.48	90°	3.7%	−2.6%	2.6%	16
Heo & Chung [10]	2094	3.73–13.2	90°	3.0%	−0.6%	2.9%	4
AlArabi & Khamis [7]	0.708	15.5–104	90°	4.0%	+0.3%	4.0%	7

5. Inclination

θ is the angle of a flat surface from vertical; $\theta = -90^\circ$ is upward-facing.

ϑ is the angle of a cylinder's axis from horizontal.

5.1 Natural Convection From an Inclined Plate. Ra is proportional to gravitational acceleration. Following the approach of Fujii and Imura [2], the Ra argument to $\bar{h}'(Ra) \equiv k \bar{Nu}'(Ra)/L'$ is scaled by $|\cos \theta|$, modeling the reduced convection of a tilted plate as a reduction in gravitational acceleration. Similarly, the Ra arguments to \bar{h}^* and \bar{h}_R are scaled by $|\sin \theta|$.

For an inclined plate, the formula in Raithby and Hollands [16] chooses the upward-facing, downward-facing, or vertical flow mode having the maximum convective surface conductance (with each Ra scaled as described above).

The upward-facing and downward-facing modes do not directly compete with each other, suggesting:

$$\bar{h} = \begin{cases} \max(\bar{h}'(|\cos \theta| Ra'), \bar{h}^*(|\sin \theta| Ra^*)) & \sin \theta < 0 \\ \max(\bar{h}'(|\cos \theta| Ra'), \bar{h}_R(|\sin \theta| Ra_R)) & \sin \theta \geq 0 \end{cases} \quad (27)$$

However, measurements of inclined plate natural convective heat transfer revealed that, in reality, the θ transition is more gradual using the ℓ^{16} -norm in Formula (28):

$$\bar{h} = \begin{cases} \|\bar{h}'(|\cos \theta| Ra'), \bar{h}^*(|\sin \theta| Ra^*)\|_{16} & \sin \theta < 0 \\ \|\bar{h}'(|\cos \theta| Ra'), \bar{h}_R(|\sin \theta| Ra_R)\|_{16} & \sin \theta \geq 0 \end{cases} \quad (28)$$

5.2 Natural Convection From an Inclined Cylinder. Flow along a flat surface is strongly constrained by that surface; competing flows combine with the ℓ^{16} -norm. Flows around an inclined cylinder are less constrained but still compete, suggesting a smaller $p > 1$.

However, natural convection flows around a long skinny cylinder will be more competitive ($p \gg 1$) than from a cylinder where $H \approx d$. This suggests combining \bar{h}^\parallel and \bar{h}^\bullet with $p = 1 + H/d$:

$$\bar{U} = \pi d H \left\| \bar{h}^\parallel(|\sin \vartheta| Ra_H), \bar{h}^\bullet(|\cos \vartheta| Ra_d) \right\|_{1+H/d} \quad (29)$$

5.3 Heo and Chung. Heo and Chung [10] measured copper electroplating onto a cylinder in a $\text{CuSO}_4/\text{H}_2\text{SO}_4$ solution. They measured the mass transfer coefficient \bar{h}_m , but reported their results as \bar{Nu}_d and \bar{Nu}_H , which scale with different characteristic lengths. The value of k was not reported, but for the purposes of comparing theory and measurements, k is arbitrary if all conversions from \bar{Nu} to \bar{h} use the same k . A value of $k = 1 \text{ mW}/(\text{m} \cdot \text{K})$ is used in Figure 5.

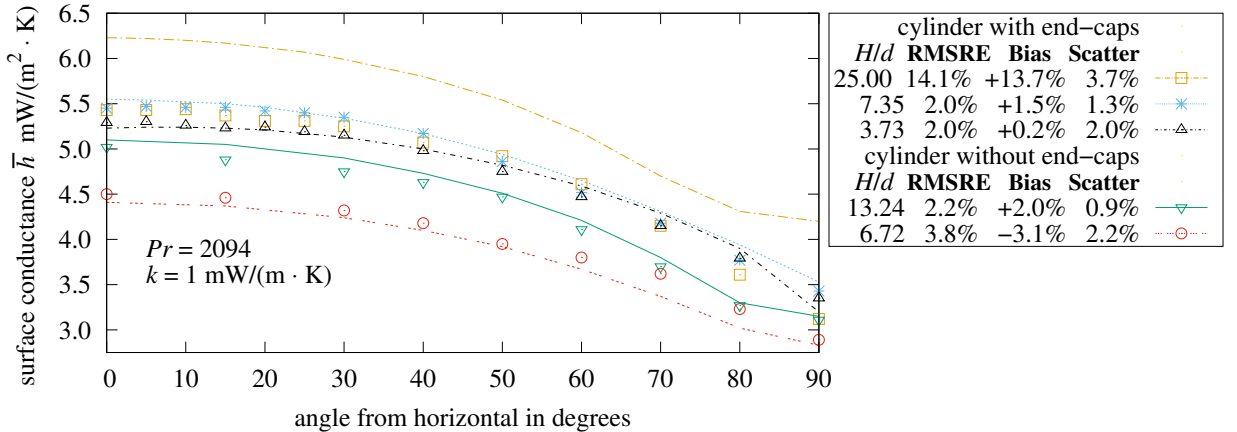


Figure 5 Heo and Chung natural convection heat transfer from inclined cylinder

The cylinder and end-caps have different areas; they must be combined as conductances. The top three rows in Figure 5 were modeled as:

$$\bar{U} + \frac{\pi d^2}{4} [\bar{h}_\uparrow + \bar{h}_\downarrow] \quad (30)$$

For the longer cylinders of the bottom two rows, \bar{h} should be the same as the shorter cylinders; but the measured \bar{h} values for $H/d = 13.24$ and $H/d = 6.72$ are significantly smaller in Figure 5. Modeling only the cylinder heat transfer, but including its end-cap areas yields $\text{RMSRE} < 4\%$:

$$\bar{h} = \frac{\bar{U}}{\pi [dH + d^2/2]} \quad (31)$$

Using their reported $Pr = 2094$, the $Ra_d = 5.07 \times 10^{10}$ in their table differs from the $Ra_d = 4.96 \times 10^{10}$ and $Gr_d = 2.37 \times 10^7$ in their figure. $Ra_d = 4.96 \times 10^{10}$ is used in the $H/d = 6.72$ and $H/d = 3.73$ curves in Figure 5.

The parameters regarding the top row are more troubling. Their table lists $Ra_d = 1.69 \times 10^8$ for the $d = 0.010$ m cylinder. Using their reported $Pr = 2094$ should result in $Gr_d = Ra_d/Pr \approx 8.07 \times 10^4$. But their figures specify $Gr_d = 6.27 \times 10^4$ and $Ra_d = 1.31 \times 10^8$ for the $d = 0.010$ m cylinder. Given these inconsistencies, the $d = 0.010$ m cylinder is omitted from this investigation's summary statistics.

5.4 AlArabi and Khamis. AlArabi and Khamis [15] measured local heat transfer to air from a “nickel-electro-plated” brass cylinder heated by steam.

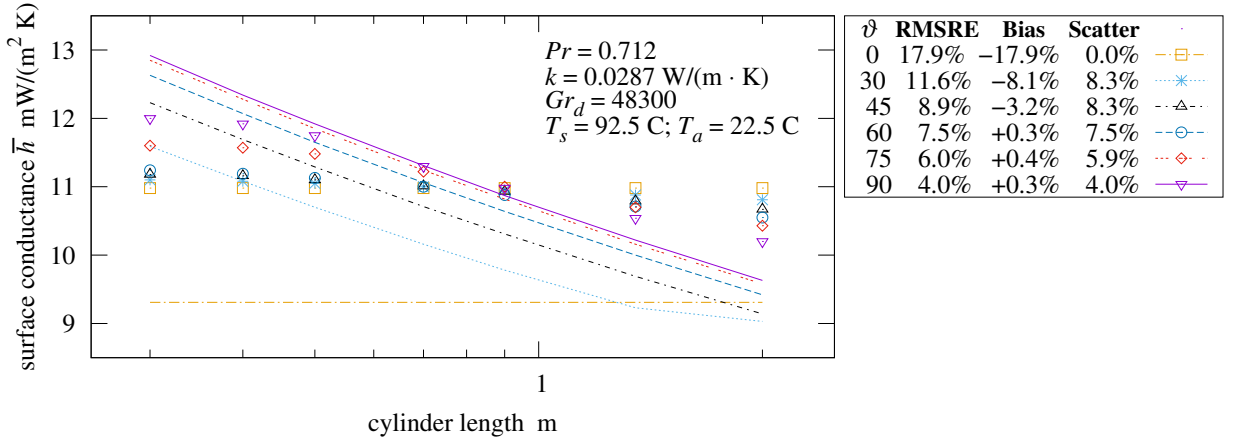


Figure 6 AlArabi and Khamis natural convection heat transfer from inclined cylinder

Text in their figures declares $Gr_d = 2.6 \times 10^4$; however, this is much smaller than the $Gr_d = 4.83 \times 10^4$ value this investigation computes from the average ambient conditions in Cairo, Egypt. This investigation uses $Gr_d = 4.83 \times 10^4$.

For the average thermal surface conductance they report h_L values instead of \bar{h} , indicating that these are a local surface conductances, not average. An earlier paper, Al-Arabi and Salman [15] reports local h_L and \bar{h} values, and claims that h_L and \bar{h} are “practically the same”. Yet this is clearly contradicted by the second figure of that paper. The only angle for which they are the same is $\vartheta = 90^\circ$.

In vertical cylinder natural convection, growth of characteristic length L corresponds to growth in the direction of fluid flow. In such systems the average heat transfer can be inferred by averaging local heat transfers h_x at lengths $0 < x \leq L$.

This fails for a horizontal cylinder because its characteristic-length is the cylinder's diameter, not its length. Figure 5 averages the h_x values to produce \bar{h} , and confirms that this averaging works only for the vertical cylinder $\vartheta = 90^\circ$. Only the vertical cylinder is included in this investigation's summary statistics.

5.5 Goldstein et al.. Goldstein et al. [9] measured copper electroplating onto three cylinders at four angles in a $\text{CuSO}_4/\text{H}_2\text{SO}_4$ solution. The cylinders were 78.8 mm in diameter and had lengths 49.9 mm, 116.4 mm, and 184.4 mm. They presented measurements without identifying the cylinder used in each trial. The present analysis treats all as having length 116.4 mm, which succeeds because the present work $0.63 \leq H/d \leq 2.34$ traces in Figure 4 are converging above $Ra/\Xi_\bullet > 10^8$.

The value of k was not reported, but for the purposes of comparing theory and measurements, k is arbitrary if all conversions from \bar{Nu} to \bar{h} use the same k . A value of $k = 1 \text{ mW/(m} \cdot \text{K)}$ is used in Figure 7.

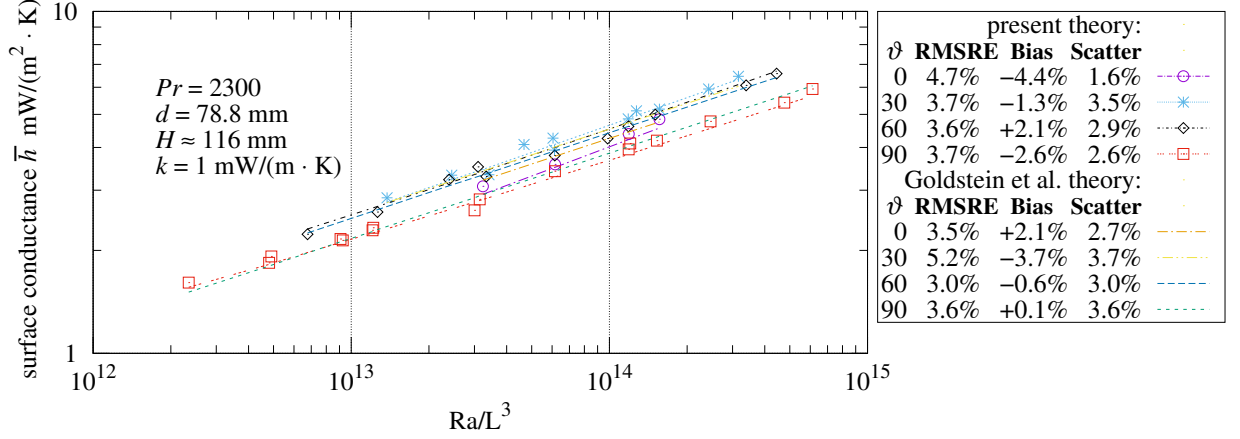


Figure 7 Goldstein et al. natural convection heat transfer from inclined cylinder

6. Discussion

Table 7 summarizes the present theory's conformance with nine data-sets from three prior works.

Table 7 Measurements versus present theory

Source	Pr or Sc	H/d	ϑ	RMSRE	Bias	Scatter	#
Goldstein et al. [9]	2300	1.48	0°	4.7%	-4.4%	1.6%	4
Goldstein et al. [9]	2300	1.48	30°	3.7%	-1.3%	3.5%	11
Goldstein et al. [9]	2300	1.48	60°	3.6%	+2.1%	2.9%	11
Goldstein et al. [9]	2300	1.48	90°	3.7%	-2.6%	2.6%	16
Heo & Chung [10]	2094	7.4	0°–90°	2.0%	+1.5%	1.3%	13
Heo & Chung [10]	2094	3.7	0°–90°	2.0%	+0.2%	2.0%	13
Heo & Chung [10]	2094	13	0°–90°	2.2%	+2.0%	0.9%	9
Heo & Chung [10]	2094	6.7	0°–90°	3.8%	-3.1%	2.2%	9
AlArabi & Khamis [7]	0.708	15.5–104	90°	4.0%	+0.3%	4.0%	7

6.1 Short Cylinders. Around a short ($H \ll d$) level cylinder the fluid flow is not restricted to the vertical plane, resulting in larger heat transfers than predicted by Formula (29). Formula (29) should work for small H/d ratios as long as H is the width of a heated band embedded in a longer, insulated cylinder as shown in Figure 8.

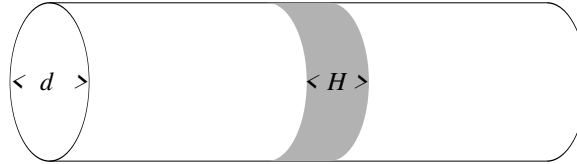


Figure 8 Cylinder with isothermal band

6.2 Non-Circular Cylinders. For a convex cylinder with hydraulic diameter d , vertical Formula (25) is expected to predict heat transfer correctly.

For a level convex cylinder, the Table 3 natural convection parameters B , D , and E may need to be reevaluated. B should be the cross-section's perimeter length squared divided by its area. D will be less than B ; for a circular cross-section $D = 2B/3$. The E (average bend) can be calculated by the method of Formulas (18) and (19).

If the cross-section lacks bilateral symmetry, then the convection may need to be calculated separately for each side of the cross-section, split along the line connecting its highest and lowest point.

6.3 Small Rayleigh Numbers. When the conduction term dominates both level and vertical modes of natural convection and $H/d \ll 1$, then Formula (29) will predict up to twice the true heat transfer because both modes have the same conduction term.

6.4 Laminar and Turbulent Flows. As stated in Section 1, the fundamental laws of thermodynamics make no distinction between laminar and turbulent flows.

Ra_d in level cylinder Formula (24) has neither the $1/4$ exponent commonly attributed to laminar flow nor the $1/3$ exponent attributed to turbulent flow, but an intermediate exponent of $1/[2 + E^\bullet] \approx 0.310$.

6.5 Rough Cylinders. Jaffer and Jaffer [17] made natural convective heat transfer measurements of a 0.305 m square plate with 3 mm root-mean-square height-of-roughness at angles between -90° and $+90^\circ$. Those measurements matched Formula (28) with 3% RMSRE, providing evidence that flat surface natural convection is insensitive to roughness which is much smaller than its characteristic length.

A similar test conducted with a rough cylinder would ascertain whether the natural convective flows from cylinders are also insensitive.

7. Conclusions

Using the thermodynamics-based analysis pioneered by Jaffer [1], this investigation derived a novel formula predicting the natural convective heat transfer from an inclined cylinder given its length H , diameter d , inclination angle ϑ , Ra_d , and the fluid's Pr and k .

The present formula was tested with 93 inclined cylinder measurements having $1.48 < H/d < 104$ at angles $0^\circ \leq \vartheta \leq 90^\circ$ in nine data-sets from three peer-reviewed studies, yielding (data-set) RMSRE values between 1.6% and 4.7%.

On 57 level cylinder measurements from Churchill and Chu [5] spanning more than 20 orders-of-magnitude of Ra , the present formula has 11% RMSRE, a significant improvement from the prior work formulas 19% and 21% RMSRE.

8. Nomenclature

B, C, D, E	dimensionless convection parameters
E^\bullet	exponent parameter for level cylinders
H	cylinder length (m)
d	cylinder diameter (m)
h_x	local convective surface conductance ($\text{W}/(\text{m}^2 \cdot \text{K})$)
\bar{h}	average convective surface conductance ($\text{W}/(\text{m}^2 \cdot \text{K})$)
\bar{h}^*	upward convective surface conductance ($\text{W}/(\text{m}^2 \cdot \text{K})$)
\bar{h}'	vertical plate convective surface conductance ($\text{W}/(\text{m}^2 \cdot \text{K})$)
\bar{h}_R	downward convective surface conductance ($\text{W}/(\text{m}^2 \cdot \text{K})$)
\bar{h}^\bullet	level cylinder convective surface conductance ($\text{W}/(\text{m}^2 \cdot \text{K})$)
\bar{h}_\uparrow	upper end-cap convective surface conductance ($\text{W}/(\text{m}^2 \cdot \text{K})$)
\bar{h}_\downarrow	lower end-cap convective surface conductance ($\text{W}/(\text{m}^2 \cdot \text{K})$)
k	fluid thermal conductivity ($\text{W}/(\text{m} \cdot \text{K})$)
L	characteristic length (m)
L^*	characteristic length of upward-facing surface (m)
L'	characteristic length of vertical surface (m)
L_R	characteristic length of downward-facing surface (m)
Nu'_0	Nusselt number of vertical plate conduction
Nu_0^*	Nusselt number of upward-facing plate conduction
Nu_0^\bullet	Nusselt number of level cylinder conduction
\bar{Nu}	average Nusselt number
\bar{Nu}^*	Nusselt number of upward-facing plate
\bar{Nu}'	Nusselt number of vertical plate plate
\bar{Nu}_R	Nusselt number of downward-facing plate
\bar{Nu}^\bullet	Nusselt number of level cylinder
Nu^\parallel	Nusselt number of vertical cylinder
p	exponent in ℓ^p -norm
Pr	Prandtl number of the fluid
Ra	Rayleigh number
Ra_d	Rayleigh number with cylinder diameter as characteristic length

Ra^*	upward Rayleigh number with characteristic length L^*
Ra_H	vertical plate Rayleigh number with characteristic length L'
Ra_R	downward Rayleigh number with characteristic length L_R
Sc	Schmidt number of the fluid
\overline{Sh}	average Sherwood number
U_0	thermal conductance of isothermal sphere in motionless uniform medium (W/K)
\overline{U}	convective thermal conductance of cylinder (W/K)

8.1 Greek Symbols.

θ	angle of the plate from vertical
ϑ	angle of the cylinder axis from horizontal
Ξ	self-obstruction factor for plates and vertical cylinders
Ξ_\bullet	self-obstruction factor for level cylinders

9. References

- [1] Aubrey Jaffer. Natural convection heat transfer from an isothermal plate. *Thermo*, 3(1):148–175, 2023, doi:10.3390/thermo3010010.
- [2] Tetsu Fujii and Hideaki Imura. Natural-convection heat transfer from a plate with arbitrary inclination. *International Journal of Heat and Mass Transfer*, 15(4):755–764, 1972, doi:10.1016/0017-9310(72)90118-4.
- [3] Stuart W Churchill and Humbert HS Chu. Correlating equations for laminar and turbulent free convection from a vertical plate. *International journal of heat and mass transfer*, 18(11):1323–1329, 1975, doi:10.1016/0017-9310(75)90243-4.
- [4] S. W. Churchill and R. Usagi. A general expression for the correlation of rates of transfer and other phenomena. *AIChE Journal*, 18(6):1121–1128, 1972, doi:10.1002/aic.690180606.
- [5] Stuart W. Churchill and Humbert H.S. Chu. Correlating equations for laminar and turbulent free convection from a horizontal cylinder. *International Journal of Heat and Mass Transfer*, 18(9):1049–1053, 1975, doi:10.1016/0017-9310(75)90222-7.
- [6] S.S. Kutateladze. *Fundamentals of Heat Transfer*. Academic Press, New York, 1963.
- [7] M. Al-Arabi and M. Khamis. Natural convection heat transfer from inclined cylinders. *International Journal of Heat and Mass Transfer*, 25(1):3–15, 1982, doi:10.1016/0017-9310(82)90229-0.
- [8] C.O. Popiel, J. Wojtkowiak, and K. Bober. Laminar free convective heat transfer from isothermal vertical slender cylinder. *Experimental Thermal and Fluid Science*, 32(2):607–613, 2007, doi:10.1016/j.expthermflusci.2007.07.003.
- [9] R.J. Goldstein, V. Khan, and V. Srinivasan. Mass transfer from inclined cylinders at moderate rayleigh number including the effects of end face boundary conditions. *Experimental Thermal and Fluid Science*, 31(7):741–750, 2007, doi:10.1016/j.expthermflusci.2006.08.001.
- [10] Jeong-Hwan Heo and Bum-Jin Chung. Natural convection heat transfer on the outer surface of inclined cylinders. *Chemical Engineering Science*, 73:366–372, 2012, doi:10.1016/j.ces.2012.02.012.
- [11] F.P. Incropera, D.P. DeWitt, T.L. Bergman, and A.S. Lavine. *Fundamentals of Heat and Mass Transfer*. Wiley, Hoboken, NJ, USA, 2007.
- [12] E. M. Sparrow and J. L. Gregg. Laminar-free-convection heat transfer from the outer surface of a vertical circular cylinder. *Transactions of the American Society of Mechanical Engineers*, 78(8):1823–1828, 02 2022, doi:10.1115/1.4014194.
- [13] Tuncer Cebeci. Laminar-free-convective-heat transfer from the outer surface of a vertical slender circular cylinder. In *Proc. Fifth Int. Heat Transfer Conf.*, volume 3, pages 15–19, September 1974.

- [14] S.M. Yang. General correlating equations for free convection heat transfer from a vertical cylinder. In *Proceedings of the International Symposium on Heat Transfer*, pages 153–159. Hemisphere Publ. Corp., Peking, 1985.
- [15] M. Al-Arabi and Y.K. Salman. Laminar natural convection heat transfer from an inclined cylinder. *International Journal of Heat and Mass Transfer*, 23(1):45–51, 1980, doi:10.1016/0017-9310(80)90137-4.
- [16] W.M. Rohsenow, J.P. Hartnett, and Y.I. Cho. *Handbook of heat transfer*. McGraw-Hill handbooks. McGraw-Hill, 1998.
- [17] Aubrey Jaffer and Martin Jaffer. Mixed convection from an isothermal rough plate. *Thermal Science and Engineering*, 8(1), 2025, doi:10.24294/tse9275.